Cell Host & Microbe, Volume *30*

Supplemental information

Characterization of the enhanced infectivity and antibody evasion of Omicron BA.2.75

Yunlong Cao, Weiliang Song, Lei Wang, Pan Liu, Can Yue, Fanchong Jian, Yuanling Yu, Ayijiang Yisimayi, Peng Wang, Yao Wang, Qianhui Zhu, Jie Deng, Wangjun Fu, Lingling Yu, Na Zhang, Jing Wang, Tianhe Xiao, Ran An, Jing Wang, Lu Liu, Sijie Yang, Xiao Niu, Qingqing Gu, Fei Shao, Xiaohua Hao, Bo Meng, Ravindra Kumar Gupta, Ronghua Jin, Youchun Wang, Xiaoliang Sunney Xie, and Xiangxi Wang

Supplemental Figure Legends

Figure S1. Receptor-binding features of Omicron variants, Related to Figure 2.

(A) Binding affinity of hACE2 with B.1.1.7 (Alpha) RBD, B.1.351 (Beta) RBD, P.1 (Gamma) RBD, B.1.617.2 (Delta) RBD, BA.1 RBD, BA.2.12.1 RBD, BA.3 RBD measured by SPR.

(B) Flow charts for cryo-EM data processing of BA.2.75 spike and hACE2 complex.

(C) Binding affinity of hACE2 with BA.2.75+H339D RBD measured by SPR.

Figure S2. Structural analyses of BA.2.75 spike in different pH, Related to Figure 3.

(A-B) Flow charts for cryo-EM data processing of BA.2.75 spike at (A) neutral pH and (B) acidic pH.

(C) Superimposition of S2 subunit of the BA.2.75 S-trimer (pH7.4, gray) onto the BA.2.75 S-trimer (pH5.5, yellow, lightblue, pink).

(D) Buried surface areas between two neighboring RBDs of WT spike.

(E) Structural organization of three RBDs from the neutral (gray) and acidic BA.2.75 S-trimer (yellow, light blue and pink).

(F) Superimposition of the neutral WT S-trimer structure (grey) onto the structure of the acidic WT S-trimer (RBD, yellow; NTD, hot pink); Structural rotations and shifts between these two structures were marked by green lines and arrows.

(G) Structural features underpinning the up configuration. Left: Cartoon representation of BA.2.75 and BA.2 S-trimer in a prefusion conformation with one protomer in “open” state. The BA.2.75 RBD and BA.2 RBD are colored in magenta and gray, respectively. The NTD domain and S2 domain are colored in yellow and cyan, respectively. The zoomed-in view of interaction details of two independent interfaces for BA.2.75 (middle panel) and BA.2 (right panel). The mutated residues are shown as sphere in red, and the residues involved in the interactions are shown as sticks. The hydrogen bonds are shown as yellow dashed lines and hydrophobic network is highlighted in gray.

Figure S3. Local conformational change of BA.2.75 RBD compared to BA.1, Related to Figure 4.

Structural comparison of α1 and α2 helices on RBDs of BA.2.75 (left) and BA.1 (right). The π-π stack formed between H339 and F371 in BA.2.75 RBD are marked as yellow dashed lines. The distances between α1 and α2 helices on RBD are also highlighted.

Figure S4. Binding affinity of S309 against Omicron variants RBD, Related to Figure 5.

(A) BLI sensorgrams measuring the binding affinity of S309 with BA.1 RBD, BA.2 RBD, BA.2.12.1 RBD, BA.4/5 RBD and BA.2.75 RBD.

(B) Neutralization curves of S309 against Omicron BA.1, BA.2, BA.2.12.1, BA.4/5, and BA.2.75 pseudovirus. Neutralization assays were conducted in two replicates.

Figure S5. Structural analyses of BA.2.75-S309 complex, Related to Figure 5.

(A) Flow charts for cryo-EM data processing of BA.2.75 spike and S309 complex.

(B) Surface presentations of the three states of BA.2.75 S-trimer in complex with S309 Fab. The three subunits of S protein are colored in yellow, cyan, and magenta, respectively. The heavy chain and light chain are colored in light pink and light seagreen, respectively.

(C) Diagram presentation of N343 glycan conformational differences among BA.1 bound to S309 (gray), BA.2 bound to S309 (pink), and BA.2 bound to BD55-5840 (blue) are shown.

Figure S6. Characteristics of NTD-targeting antibodies, Related to Figure 7.

(A) Heatmap of pseudo-typed virus neutralization by antibodies recognized NTD (unit: μg/ml).

(B) Analysis of sequence conservation of four classes (α, β, γ and δ) epitopes of NTD recognized antibodies. The logo plot represents the conservation of epitopes residues from 26 SARS-CoV-2 lineages: WT, Alpha, Beta, Gamma, Lambda, Mu, Delta, Delta plus, BA.1, BA.1.1, BA.2, BA.2.12.1, BA.2.13, BA.4, BA.5, BA.2.75, Eta, Lota, Kappa, Theta, Iota, B.1.1.318, B.1.620, C.1.2, C.363 and Epsilon. Deletions on NTD are represented as red triangles.

(C) Heatmap represents the frequency of NTD residues recognized by NAbs from four classes (α, β, γ and δ). Mutations present in BA.2.75 NTD are marked out and highlighted.

Figure S7. Cryo-EM structures of BA.2.75 spike in complex of XG2v024, Related to Figure 7.

Flow charts for cryo-EM data processing of BA.2.75 spike and XG2v024 complex.

Figure S1

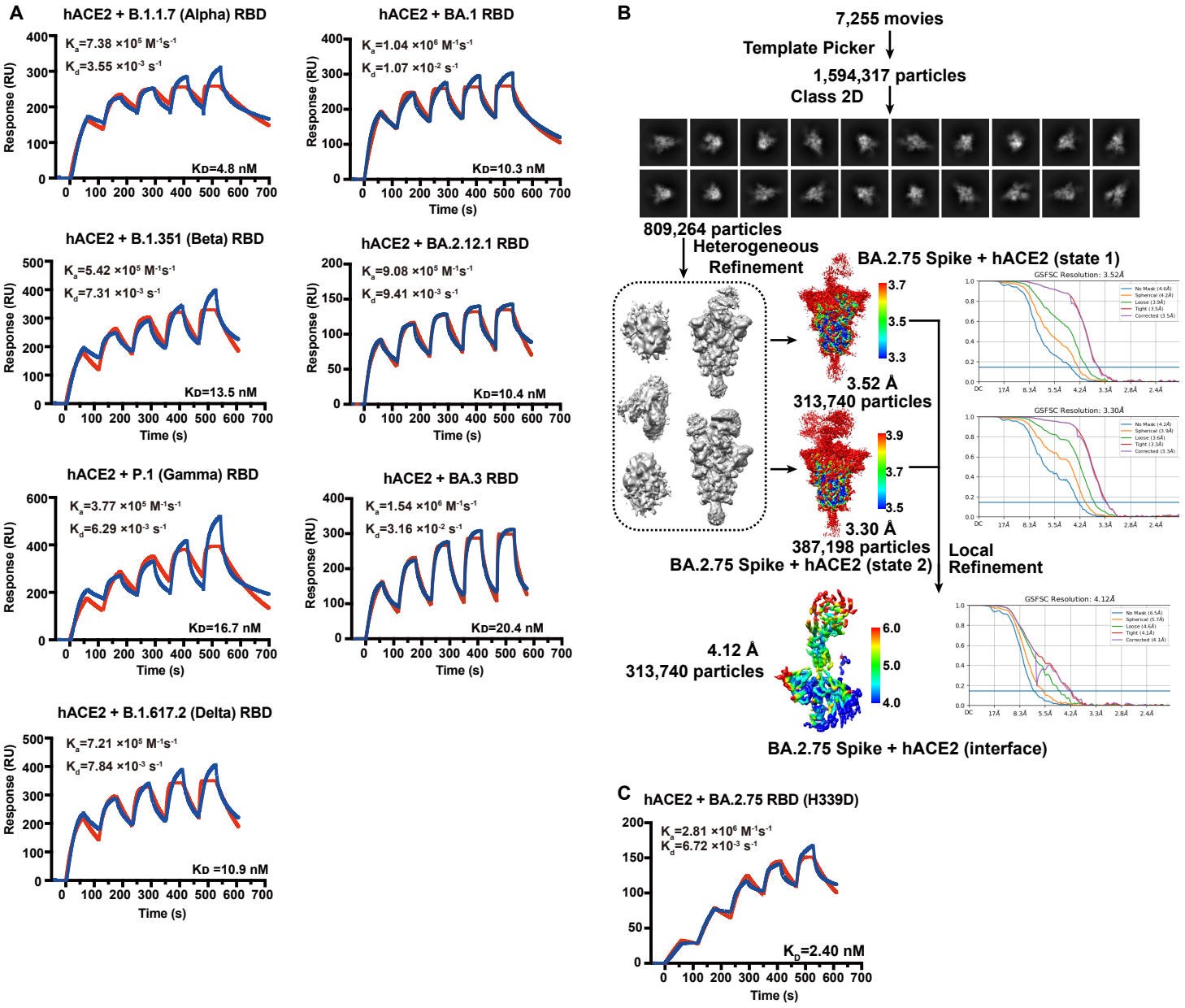

Figure S1. Receptor-binding features of Omicron variants, Related to Figure 2.
(A) Binding affinity of hACE2 with B.1.1.7 (Alpha) RBD, B.1.351 (Beta) RBD, P.1 (Gamma) RBD, B.1.617.2 (Delta) RBD, BA.1 RBD, BA.2.12.1 RBD, BA.3 RBD measured by SPR.
(B) Flow charts for cryo-EM data processing of BA.2.75 spike and hACE2 complex.
(C) Binding affinity of hACE2 with BA.2.75+H339D RBD measured by SPR.

Figure S2

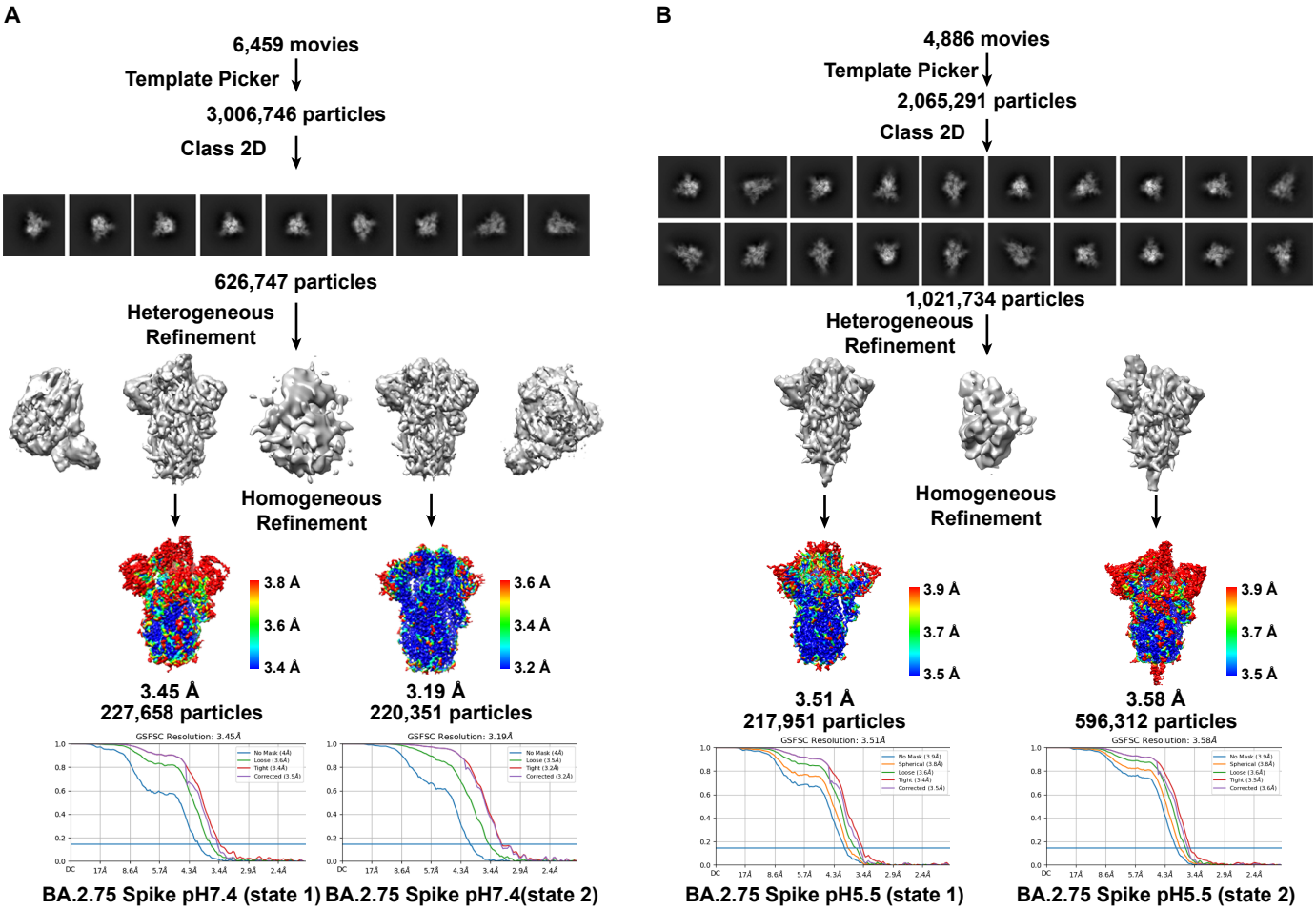

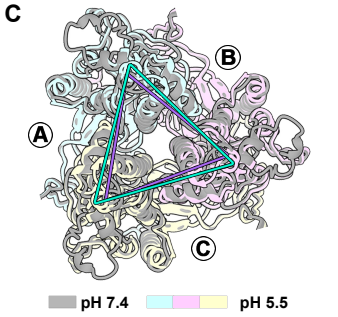

D

		AB (Å²)	BC (Å²)	CA (Å²)	AVE. (Å²)	Fold Change
WT RBD	pH 7.4 (6ZB5)	514	513	515	514	1.8
	pH 5.5 (6XM5)	255	246	352	284	

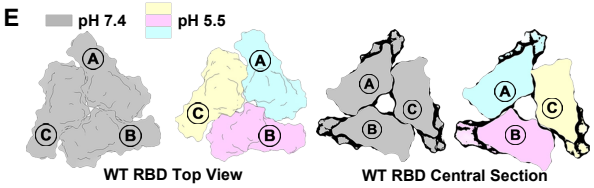

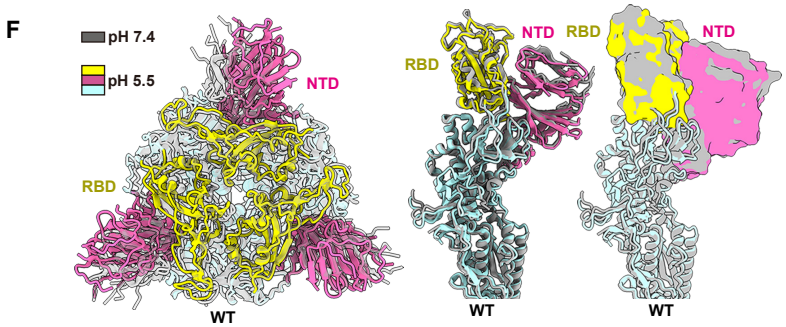

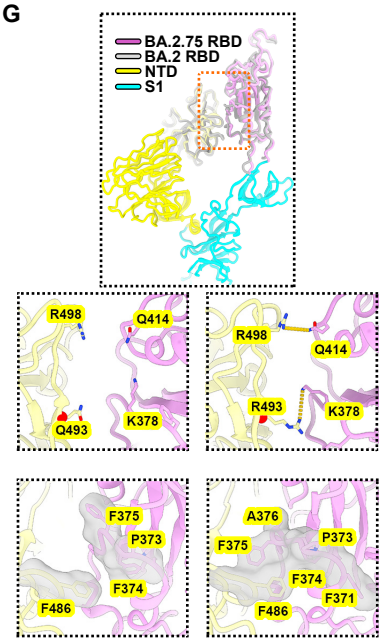

Figure S2. Structural analyses of BA.2.75 spike in different pH, Related to Figure 3.
(A-B) Flow charts for cryo-EM data processing of BA.2.75 spike at (A) neutral pH and (B) acidic pH.
(C) Superimposition of S2 subunit of the BA.2.75 S-trimer (pH7.4, gray) onto the BA.2.75 S-trimer (pH5.5, yellow, lightblue, pink).
(D) Buried surface areas between two neighboring protomers of WT spike.
(E) Structural organization of three RBDs from the neutral (gray) and acidic BA.2.75 S-trimer (yellow, light blue and pink).
(F) Superimposition of the neutral WT S-trimer structure (grey) onto the structure of the acidic WT S-trimer (RBD, yellow; NTD, hot pink); Structural rotations and shifts between these two structures were marked by green lines and arrows.
(G) Structural features underpinning the up configuration. Left: Cartoon representation of BA.2.75 and BA.2 S-trimer in a prefusion conformation with one protomer in “open” state. The BA.2.75 RBD and BA.2 RBD are colored in magenta and gray, respectively. The NTD domain and S2 domain are colored in yellow and cyan, respectively. The zoomed-in view of interaction details of two independent interfaces for BA.2.75 (middle panel) and BA.2 (right panel). The mutated residues are shown as sphere in red, and the residues involved in the interactions are shown as sticks. The hydrogen bonds are shown as yellow dashed lines and hydrophobic network is highlighted in gray.

Figure S3

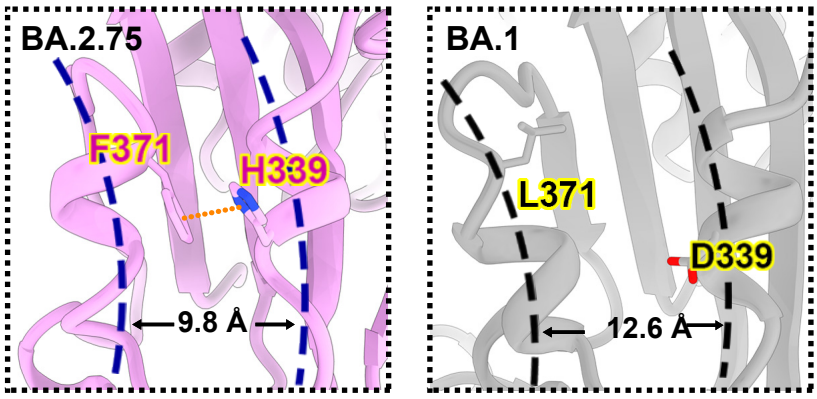

Figure S3. Local conformational change of BA.2.75 RBD compared to BA.1, Related to Figure 4.
Structural comparison of α1 and α2 helices on RBDs of BA.2.75 (left) and BA.1 (right). The π-π stack formed between H339 and F371 in BA.2.75 RBD are marked as yellow dashed lines. The distances between α1 and α2 helices on RBD are also highlighted.

Figure S4

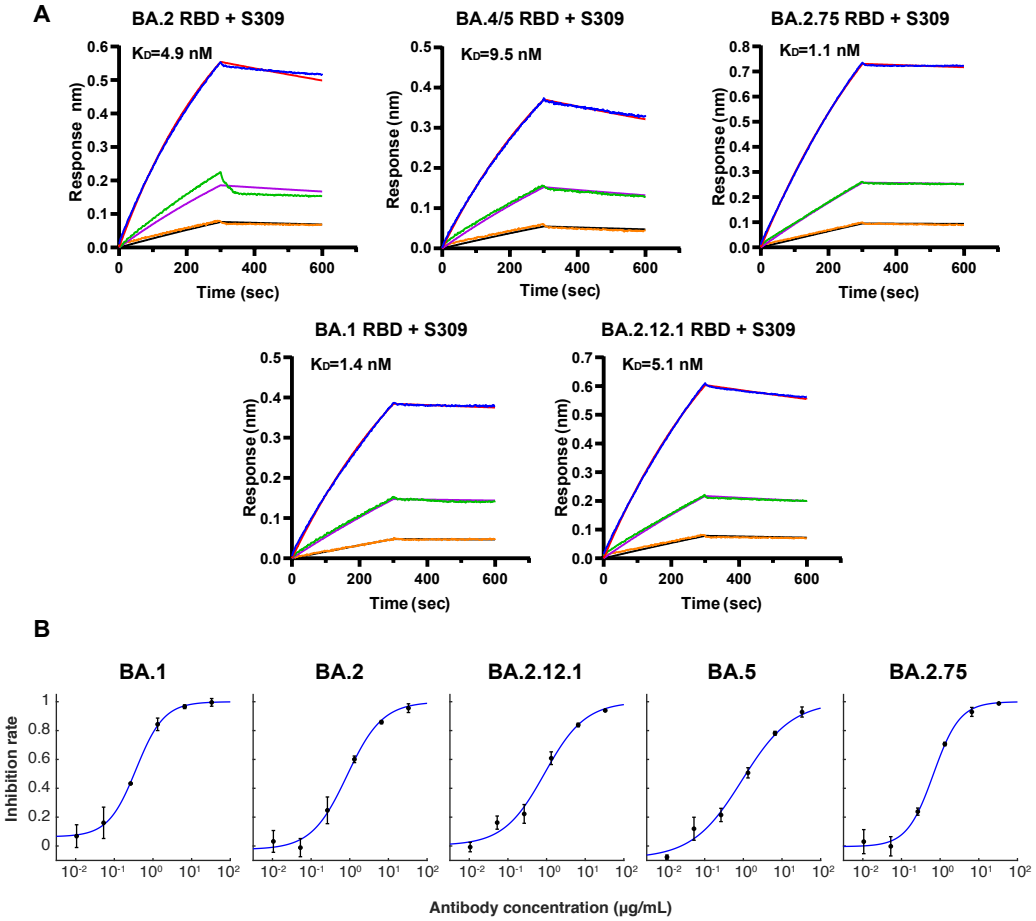

Figure S4. Binding affinity of S309 against Omicron variants RBD, Related to Figure 5.
(A) BLI sensorgrams measuring the binding affinity of S309 with BA.1 RBD, BA.2 RBD, BA.2.12.1 RBD, BA.4/5 RBD and BA.2.75 RBD.
(B) Neutralization curves of S309 against Omicron BA.1, BA.2, BA.2.12.1, BA.4/5, and BA.2.75 pseudovirus. Neutralization assays were conducted in two replicates.

Figure S5

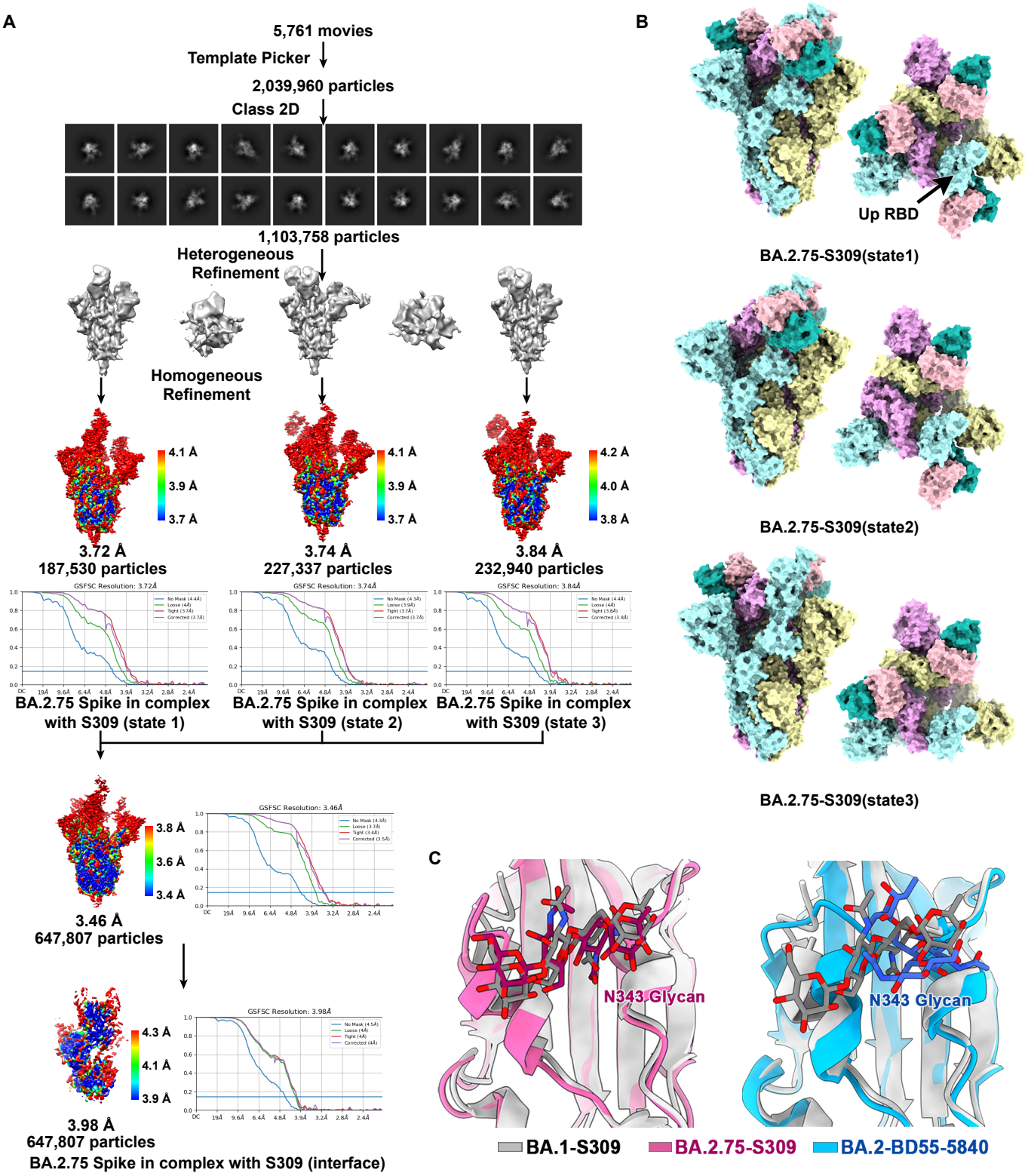

Figure S5. Structural analyses of BA.2.75-S309 complex, Related to Figure 5.
(A) Flow charts for cryo-EM data processing of BA.2.75 spike and S309 complex.
(B) Surface presentations of the three states of BA.2.75 S-trimer in complex with S309 Fab. The three subunits of S protein are colored in yellow, cyan, and magenta, respectively. The heavy chain and light chain are colored in light pink and light seagreen, respectively.
(C) Diagram presentation of N343 glycan conformational differences among BA.1 bound to S309 (gray), BA.2 bound to S309 (pink), and BA.2 bound to BD55-5840 (blue) are shown.

Figure S6

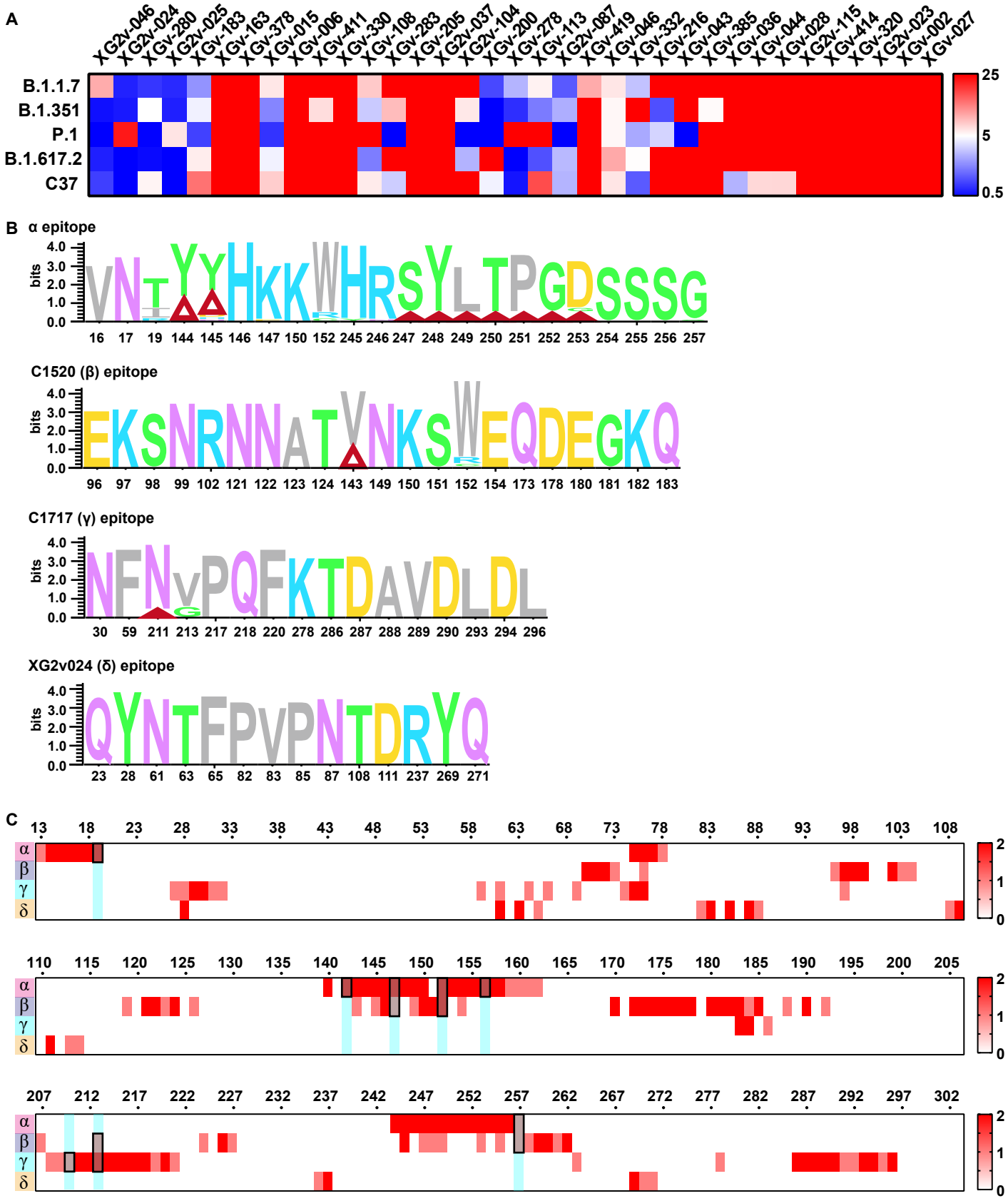

Figure S6. Characteristics of NTD-targeting antibodies, Related to Figure 7.

(A) Heatmap of pseudo-typed virus neutralization by antibodies recognized NTD (unit: μg/ml).

(B) Analysis of sequence conservation of four classes (α, β, γ and δ) epitopes of NTD recognized antibodies. The logo plot represents the conservation of epitopes residues from 26 SARS-CoV-2 lineages: WT, Alpha, Beta, Gamma, Lambda, Mu, Delta, Delta plus, BA.1, BA.1.1, BA.2, BA.2.12.1, BA.2.13, BA.4, BA.5, BA.2.75, Eta, Lota, Kappa, Theta, Iota, B.1.1.318, B.1.620, C.1.2, C.363 and Epsilon. Deletions on NTD are represented as red triangles.

(C) Heatmap represents the frequency of NTD residues recognized by NAbs from four classes (α, β, γ and δ). Mutations present in BA.2.75 NTD are marked out and highlighted.

Figure S7

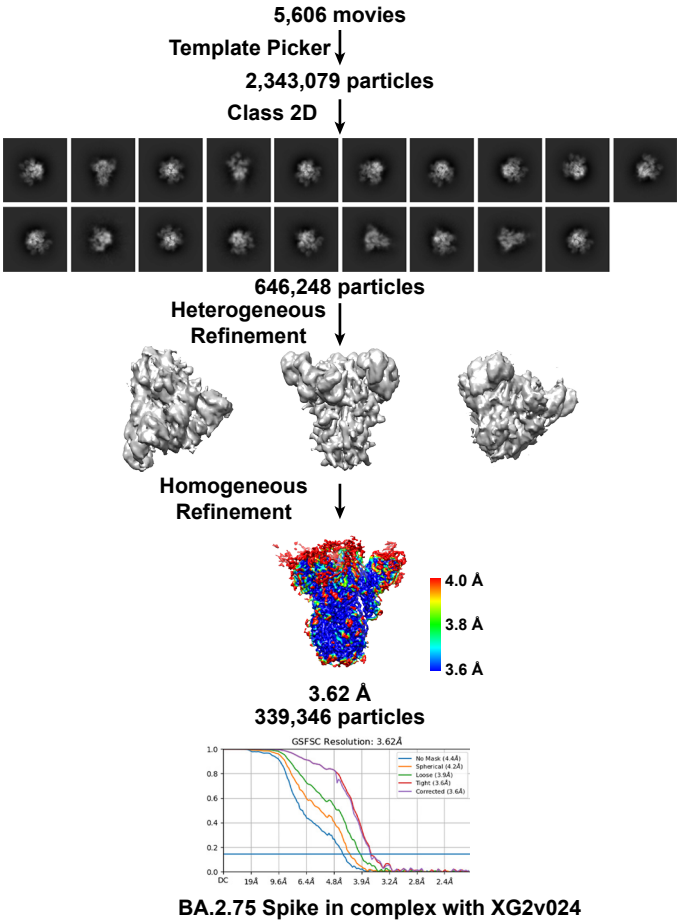

Figure S7. Cryo-EM structures of BA.2.75 spike in complex of XG2v024, Related to Figure 7.
Flow charts for cryo-EM data processing of BA.2.75 spike and XG2v024 complex.